Development of versatile Human *In Vitro* Vascularized Adipose Tissue Model with Serum-Free Angiogenesis and Natural Adipogenesis Induction

Running title: Human Vascularized Adipose Tissue Model

Outi Huttala[1*], Maaria Palmroth[1], Pauliina Hemminki[1], Tarja Toimela[1], Tuula Heinonen[1], Timo Ylikomi[1,2], Jertta-Riina Sarkanen[2]

[1] FICAM, Faculty of Medicine and Life Sciences, University of Tampere, Finland

[2] Cell Biology, Faculty of Medicine and Life Sciences, University of Tampere, Finland

*****Corresponding author

Corresponding author details: Outi Huttala, address: Faculty of Medicine and Life Sciences, University of Tampere, Arvo Ylpön katu 34, 33520 Tampere, Finland. e-mail: outi.huttala@uta.fi

Keywords: Adipogenesis, Angiogenesis, Endocrine toxicology, in vitro cell assay, In vitro toxicology and alternatives, Tissue engineering, Toxicological methods

Conflict of interest statement

Sarkanen JR and Ylikomi T have a patent issued in USA (US 20110151005 A1) and pending application (WO2010026299A1). Other authors have no conflict of interest to declare.

Abstract

Many adipose tissue related diseases, such as obesity and type 2 diabetes, are worldwide epidemics. For studying these diseases relevant human cell models are needed.

In this study, we developed a vascularized adipose tissue model where human adipose stromal cells (hASC) and human umbilical cord vein endothelial cells (HUVEC) were co-cultured with natural adipogenic and defined serum-free angiogenic media for 14 days. Several different protocols were compared to each other. The protocols varied in cell numbers and plating sequences. Lipid accumulation was studied with Adipored reagent, relative cell number with WST-1 reagent, gene expression of *glut4*, *leptin*, *adipocyte protein 2* (*aP2)*, *adiponectin*, *PPARγ* and *PPARγ2* with RT-qPCR. Secretion of adiponectin, leptin and aP2 was analyzed with ELISA. The immunostained vascular network was imaged with Cell-IQ and area quantified using ImageJ.

In this study, both angiogenesis and adipogenesis were successfully induced. Protocols produced strong lipid accumulation, good vascular network formation and induced adipocyte specific protein secretion and expression of studied adipocyte genes. Results showed that cell numbers and cell plating sequences are important factors when aiming at *in vitro* standardized tissue model. Presence of mature vasculature appeared lead to faster maturation of adipocytes judged by the lipid accumulation and gene expression results.

The developed vascularized adipose tissue model is simple to use, easily modifiable to suit various applications and as such, a promising new tool for adipose tissue research when e.g. studying the effect of different cell types on adipose tissue function or for mechanistic studies.

Introduction

Interest in studying adipose tissue and its functions is growing along with the growing prevalence of obesity and the many adipose tissue related diseases, such as type 2 diabetes mellitus, which is already a worldwide epidemics [1]. Many experimental animal models have been developed to study diabetes [2] but due to species-specific differences the results from the animal models although they increase the understanding of the mechanisms behind diseases and adverse effects, are weakly transferable to human situations [2-4]. Also, due to new regulations which promote and demand replacement of animal experiments, more human biology mimicking in vitro experiment models are needed. Examples of such as are Directive 2010/63/EU [5], the cosmetics regulations [6] and the EU chemicals legislation REACH [7].

More than being the energy storage, adipose tissue is an active endocrine organ, which is particular closely associated with vascular system. Enlargement of the adipose tissue can be supported by new blood vessel formation, neovascularization, or by dilating and remodeling of the already existing capillaries [8]. Mouse studies have shown that induction of vessel expansion in obese mice counteract obesity and related metabolic complications [9] but also contrary results have been obtained as inhibition of vessel formation by an anti-angiogenic drug decreased fat pad weights of normal mice by 12 - 22 % and decrease their body weights in a dose-dependent and reversible manner [10].

Two different angiogenesis triggers in *in vivo* adipose tissue expansion have been proposed: 1) angiogenesis is a response to hypoxia, which is caused by the enlargement of adipocytes and/or proliferation of adipocytes or 2) angiogenesis is a result of developmental and/or metabolic signals in adipose tissue, i.e. blood vessels develop in

parallel or before the adipose tissue expansion [11]. There are several studies supporting the role of hypoxia [11-13]. However, in fetal development, angiogenesis/vasculogenesis precedes adipogenesis and blood vessel extracellular matrix (ECM) develops before adipose tissue ECM development [14]. The reciprocal interaction between ECM stroma and vascular network has also been shown to be important in directing vessel growth [15-17].

Current human cell in vitro vascularized adipose tissue models are based on 1) culturing human stromal cells (hASC) and human umbilical cord vein endothelial cells (HUVEC) on a scaffold such as porous silk protein scaffold [18] or 2) culturing human preadipocytes with human endothelial cells in a fibrin glue matrix on a chick chorioallantoic membrane [19,20] or 3) by adding multiple different cell types into the culture [21]. While these models are mimicking vascularized adipose tissue, they are complex, require long culture times and are laborious to be transferred into routine use. In addition, the additional components such as biomaterial scaffolds may interfere with the cell-cell interactions or cause unwanted and unknown interactions between material and the studied cells or chemicals [22-24].

The aim of this study was to develop a robust human vascularized adipose tissue model without artificial scaffold. Such model could be utilized in basic adipose tissue research, for drug discovery and safety studies, and it could also be modified to disease model, which could be used in studies of disease pathogenesis, development of intervention therapeutics and screening of personalized therapeutics. In the model we used hASC and HUVEC to form co-culture in which adipogenesis was induced by the novel natural adipogenesis inducer ATE [25] and angiogenesis by our previously developed defined serum-free angiogenesis medium [26]. The defined serum-free angiogenesis medium

produces mature vascular structures *in vitro* [26] and this medium together with ATE differentiates hASC to insulin-sensitive adipocytes [27]. In this work we compared several protocols to find the most optimal for formation of vascularized adipose tissue bearing in mind the use of the model as a routine standard model. The formed vascularized adipose tissue was characterized for morphology, lipid accumulation, secretion of adiponectin, leptin and adipocyte protein 2 (aP2, also known as fatty acid-binding protein 4) and the mRNA expression of *glut4*, *leptin*, *aP2*, *adiponectin*, *PPARγ* and *PPARγ2*. The findings of this article present two protocols, which are both easy-to-use, adjustable for different applications and relevant for culturing a vascularized adipose tissue cell model.

Materials and Methods

Development strategy

Six different protocols (Table 1) were compared to each other for their capability to create vascularized adipose tissue. The studied protocols had following variables: cell number, cell plating time point (on day 1 or on two separated days, i.e. on days 1 and 7) and the differentiation process (adipogenesis induced prior to angiogenesis or vice versa). Adipogenesis was induced with the ATE and angiogenesis with the defined serum-free angiogenesis medium. Adipogenesis is induced with ATE medium and angiogenesis with Angiogenesis medium. Three types of controls were used (Table 1) negative control with no induction, vasculature control in which only angiogenesis was induced and adipocyte control in which only adipogenesis was induced.

Isolation and culture of human adipose stromal cells and umbilical cord vein endothelial cells

The human adipose tissue samples and umbilical cords were obtained from Tampere University Hospital, Tampere, Finland, with individual written informed consent. The use of ATE, hASC and HUVEC were approved by the Ethics Committee of the Pirkanmaa Hospital District, Tampere, Finland with permit numbers R03058 and R08028, respectively.

hASC were isolated using collagenase I (Gibco) as described previously [26,28]. HUVEC were isolated by cannulating the umbilical cord vein and infusing the vein with collagenase I (Gibco) and cultured in Endothelial Cell Growth Medium (EGM-2, Lonza) as described earlier [26,28]. Possible mycoplasma contamination was tested with MycoAlert® Detection Kit (Lonza) from both cells before cryopreservation.

hASC-HUVEC co-culture plating and differentiation protocols to form vascularized adipose tissue

In order to find out the optimal plating time for hASC and HUVEC with respect to the differentiation of the cells into adipocytes and blood vessels, six different protocols were compared to each other (Table 1). On day 0, hASC (p1) were seeded in Endothelial Cell Growth Medium (Lonza) at 20 000 cells/cm^2 or 40 000 cm^2 on 48-well Nunclon™ Δ-Surface (Sigma Aldrich) plates. In some protocols there was addition of hASC on day 7 (Table 1) in 50µl of medium without changing the medium in the well. HUVEC (p3) were seeded on top of hASC in 50µl at 4000 cells/cm^2 either on day 0 or on day 7 depending on the plating strategy (Table 1). Three different hASC-HUVEC combinations were used and all strategies were tested with all of the hASC-HUVEC combinations.

hASC-HUVEC co-cultures were exposed to adipogenic ATE medium [25] or angiogenesis medium [26] on day 1. ATE was prepared as described earlier [27]. Composition of all media used in the study are listed in Table 2. Vasculature control was exposed only to angiogenesis medium, adipocyte control only to ATE medium and negative control (undifferentiated cells) to serum-free medium (Table 1). Differentiation media were changed on days 4, 8 and 11.

Analysis of the co-culture

All analyses of the cultures were performed on day 14.

Analysis of secreted proteins

Media samples were analyzed for their concentration of Adiponectin, Leptin and aP2 with Quantikine ELISA (R&D Systems) according to manufacturer's instructions. Absorbance was measured at 450nm and 540nm.

Relative cell number

The relative cell number was defined using Cell proliferation reagent WST-1 (Roche Diagnostics, Basel, Switzerland) according to manufacturer's instruction by incubating the reagent for 1 hour and measured at 450 nm by multipoint measurement.

Lipid accumulation

The lipid accumulation was determined using Adipored assay reagent (Lonza) according to manufacturer's instructions from the same wells from which the WST-1 staining was performed. The fluorescence was measured by multipoint measurement with Varioskan flash multimode reader (Thermo Fischer Scientific) with excitation at 485 nm and emission at 572 nm.

Immunocytochemical stainings

To visualize and analyze the formed vasculature, immunocytochemical stainings were performed. For this, the same cell cultures, which were used for Adipored and WST-1 measurements, were stained.

Cells were fixed with 4 % formaldehyde (Thermo Fisher Scientific) at RT for 20 min and treated with 0.5 % Triton-X100 (MP Biochemicals, Santa Ana, CA, USA) at RT for 15 min and with 10 % bovine serum albumin (BSA, Roche Diagnostics) at RT for 30 minutes. Primary antibodies; von Willebrandt factor IgG (anti-vWf IgG produced in Rabbit, #F3520, Sigma Aldrich; 1:100), and Anti-Collagen IV IgG (anti-ColIV IgG produced in mouse, #C1926, Sigma Aldrich, 1:500), diluted in 1 % BSA in DPBS were and incubated for 1h at RT or overnight at +4ºC. Cells were then incubated for 40 minutes at RT with secondary antibodies diluted in 1% BSA in DPBS; FITC-labeled goat polyclonal antibody anti-mouse IgG (Sigma Aldrich, 1:100), and TRITC-labeled goat polyclonal antibody anti-rabbit IgG (Sigma Aldrich, 1:50).

Microscopic analyses

Vasculature and lipid accumulation were imaged with Nikon Eclipse Ti-S inverted fluorescence microscope (Nikon, Tokyo, Japan) and Nikon digital sight DS - U2 camera (Nikon). Images were processed with NIS Elements (Nikon) and Adobe Photoshop CS3 software (Adobe Systems Incorporated, San Jose, CA, USA).

Quantification of vasculature

To determine the area of vasculature, immunostained cells were imaged with Cell-IQ (CM Technologies Oy, Tampere, Finland) with 10x objective with grid of 5x5. Images were stitched together with Cell-IQ Analyzer (CM Technologies Oy) and further

analyzed with ImageJ software (The National Institutes of Health, Maryland, USA). Images were converted to 8-bit gray scale and the background was subtracted. Then, binary threshold function was adjusted to separate the tubules from background staining. The total tubule area was calculated as the total number of pixels in images with a set threshold. Results were plotted in GraphPad Prism (GraphPad Software Inc). *n* was 12 for negative control, adipocyte control, vasculature control and P1 and P5. For protocols 2 and 6, *n* was 5. Results are depicted as mean± standard deviations.

Gene expression

The cells were lysed with the lysis buffer from Purelink RNA Minikit (Life Technologies) so that parallel sample cells from five to eight wells were lysed into 600 µl of the lysis buffer and combined as one sample. Isolation was continued according to the instructions of the Purelink RNA Minikit (Life Technologies). The 260/280 purity ratios were measured with µPlate (Thermo Fischer) and Varioskan flash multimode reader (Thermo Fischer). Genomic DNA contaminations were eliminated with Purelink DNAse treatment (Life Technologies). The quality of RNA samples was checked using QIAxcel RNA QC kit v2.0 (Qiagen, Venlo, Netherlands) and QIAxcel Advanced (Qiagen). cDNA was synthetized with iScript cDNA synthesis kit (Biorad, CA, USA) according to the protocol of the manufacture. cDNAs were then preserved at -80ºC until RT-qPCR.

qPCR to study mRNA expression of *PPARγ, PPARγ2, Adiponectin, Leptin, aP2* and *Glut4*, was performed with CFX96 Real-Time System (Biorad) and with iQ™ SYBR® Green supermix (Biorad). These gene markers were chosen according to our previous study [27] and to represent markers of different stages of adipocyte differentiation. The specificity of the primer sequences was tested with NCBI/ Primer-BLAST. Primer concentration was 300nM and amount of template was 30 ng. Thermal cycling conditions

were as follows: 95 ºC 3 min, 95 ºC 10 sec, 51 - 65 ºC (gradient) 15 sec, 72ºC 30 sec, repeated 40 times. Melt Curve analysis was performed at 55 - 95 ºC (0.5 ºC increment/10 sec). Used housekeeping genes and adipocyte marker genes are listed in Table 3. The quality of amplified DNA was studied with gel electrophoresis using High Sensitivity DNA analysis kit (Agilent Technologies, Santa Clara, California, USA) and Agilent 2100 Bioanalyzer (Agilent Technologies) according to manufacturer's instructions.

Data handling and statistical analyzes

Quantification of lipid accumulation

To achieve a lipids/cell value, normalized Adipored assay absorbance values were divided with mean WST-1 assay absorbance values for the protocol in question. Normalization and Adipored/WST-1 ratio calculations were made with Microsoft Excel 2013 (Microsoft Corporation, Redmond, Washington, USA). n was 12.

Quantification of secreted leptin, aP2 and adiponectin

From the ELISA analysis, protein concentration results were obtained by subtracting the 540nm reading from the 450nm absorbance values, creating the standard curve and calculating the concentrations of the studied proteins. These results were then divided by the relative cell number i.e. WST-1 results. In ELISA samples, adipocyte control and P2 and P6 contain cytokine rich ATE and hence the protein concentrations are compared to each other. Similarly, negative control, P1 and P5 were compared to each other. *n* was 3.

RT-qPCR result quantification

qPCR data was analyzed using CFX96 Real-Time System software (Biorad). The relative quantification of mRNA expression data was calculated using ΔCt –method with Microsoft Excel 2013 (Microsoft Corporation) with the following equation:

$2^{(Ct(\text{mean of housekeeping genes SDHA and 36B4, studied protocol})-Ct(\text{Gene of interest, studied protocol}))}/$

$2^{(Ct(\text{mean of housekeeping genes SDHA and 36B4, control})-Ct(\text{Gene of interest, control}))}$

For the expression analysis, Adipocyte control was used as control. Four biological replicates of each strategy were analyzed (n=4).

Statistics

All results were plotted and statistical analyzes were performed with GraphPadPrism (GraphPad Software Inc., California, USA). Results are depicted as mean± standard deviation. Results from lipid accumulation, Cell-IQ image analysis and RT-qPCR were subjected to one-way analysis of variance (ANOVA), followed by Tukey's multiple comparison test. Results for protein secretion were subjected to one-way analysis of variance (ANOVA), followed by Sidak's multiple comparison test. Differences were considered significant when *$p<0.05$, **$p<0.01$ and ***$p<0.001$.

Results

Practical considerations

Cell detachment occurred when high number of cells was plated at once on the same day, i.e. in protocols P3 and P4 (Table 1). Due to this issue, those protocols were omitted from further analyses even though both produced dense tubule network and evenly distributed adipored staining. All other protocols (P1, P2, P5 and P6) were analyzed further. When the same number of cells was plated on two separate days (P1 and P2), i.e. half on day one and other half on day 7, no detachment was observed from the culture vessel during the 14 day culture. However, P2 and P6, in which angiogenesis was induced prior to adipogenesis, were found to detach from the culture vessel easier than P1 and P5 during handling the cultures.

Lipid accumulation

Cultures were stained with Adipored lipid dye on day 14. The lipid accumulation was strong and evenly distributed throughout the culture in all studied protocols (P1, P2, P5 and P6), including the adipocyte control (Fig 1). Negative control and vasculature control showed only slight staining with Adipored (Fig 1).

Lipid accumulation was quantified by calculating the ratio between the normalized Adipored values and WST-1 values giving relative lipids/cell value (Fig 2). Adipocyte control ($p=0.0021$) and protocol P6 ($p=0.0008$) accumulated significantly more lipids than negative control. P5 accumulated significantly less lipids than adipocyte control ($p=0.0253$). P6 accumulated significantly more lipids than P2 ($p=0.0455$) and P5 ($p=0.0091$).

Formation of vasculature

Vasculature was visualized with immunocytochemical stainings, imaged, and the area covered by tubules was quantified. Figure 1 presents the morphology of vasculature for protocols P1, P2, P5 and P6. Branched vascular networks were obtained in vasculature control as well as in all protocols but were not observed in the negative control or in the adipocyte control. The networks were more dense and more branched when they had 14 days to mature (in vasculature control, as well as in P2 and P6) compared to those in P1 and P5, which had 7 days to differentiate (Table 1). The stainings showed intact outer basement membrane (collagen IV) and inner endothelial layer (vWf) in all of the samples (Fig 1). The width of the formed vascular structures in tubule control and in different strategies did not differ markedly from each other as observed with microscope.

The area of the vascular networks was quantified from Cell-IQ images with ImageJ (Fig 2). Out of the studied protocols (P1, P2, P5 and P6; Table 1), P1 was the only studied protocol which produced significantly less tubules than vasculature control ($p=0.0012$). However, P1 also contained adequate vascular network as seen in Fig 1, although not as extensive as in other protocols.

Secretion of adipocyte specific proteins

ELISA was performed for quantification of adipocyte specific proteins in the samples collected from the culture media on day 14 (Fig 3). Medium of adipocyte control, P2 and P6 contained cytokine rich ATE, and hence these medium samples were compared to each other. Samples from P1 and P5 did not contain ATE and they were compared to the negative control, which contained the same basal medium as the protocols did.

Secretion of adiponectin was significantly increased in P6 compared to adipocyte control and P2 ($p=0.0062$ and $p=0.0011$, respectively). Also aP2 secretion was significantly increased in protocol P6 compared to adipocyte control and P2 ($p=0.0024$ and $p=0.0002$, respectively). Significantly more leptin was secreted in P1 ($p=0.0001$) and P5 ($p<0.0001$) than in the negative control. Leptin secretion was also significantly higher in protocol P6 than in P2 ($p=0.0150$).

The adipocyte specific mRNA expression in the formed adipose tissue

Expression of marker genes *PPARγ, PPARγ2, aP2*, *adiponectin*, *leptin* and *Glut4* was investigated on day 14. *PPARγ, PPARγ2, leptin, aP2* and *glut4* were shown to be expressed in P1, P2, P5 and P6 and there was no significant difference in the expression between the studied protocols and adipocyte control (Fig 4). *Adiponectin* expression was

significantly higher in P1 adipocytes when compared to adipocyte control (p=0.0115) or P5 (p=0.0357). The expression of *PPARγ* and *PPARγ2* showed a trend that when general *PPARγ* was expressed at high level, *PPARγ2* was expressed at low level and vice versa. The gene expression results (Fig 4) are given as relative expression using adipocyte control as control.

Discussion

In this study, we developed a human relevant vascularized adipose tissue model aiming at standardized artificial scaffold free test for routine use. The used human adipose tissue derived extract (ATE) induce adipogenesis in hASC culture [25] and the vascular network was constructed as published earlier by Huttala et al. [26]. ATE has been found to be a superior inducer of adipogenesis over the commonly used chemical induction cocktail [25]. The vascular network, induced by serum-free angiogenesis medium, has also been characterized earlier and found to produce optimal, *in vivo* like vascular structures [26]. Six different protocols were studied and characterized in this study. They were evaluated by their reproducibility and their ability to induce adipocyte specific marker expression in the cultures. Simultaneously the effect of the vasculature on the adipogenesis was assessed.

Adipogenesis and angiogenesis were both successfully induced, although differences were seen between the protocols in triglyceride accumulation and in density of vascular networks. The results showed that dense vasculature which existed before start of adipogenesis induction, helped the preadipocytes mature faster. Different cell plating and differentiation protocols had a notable effect on the resulting cell model and its technical repeatability. The most optimal protocols based on triglyceride accumulated, sufficient

vascular network formation and relevant adipocyte specific genes and protein expression for building the vascularized adipose tissue model were P1 and P6 (Table 1). These protocols are scaffold-free and they are simpler and demand shorter culture time than other existing vascularized adipose tissue models [18-21]. Due to the simplicity of these two protocols; two cells and two induction medias, they can also be easily modified to suit the various applications e.g. effect of third cell type on adipose tissue metabolism.

Vasculature formation in different protocols

Dense vascular networks were induced with all protocols and the vasculature has been shown to be mature in 7 days [26]. Apart from the angiogenesis induced with the stimulation medium, the adipogenesis inductor, ATE, has also been shown to induce angiogenesis [25]. Thus, the ATE treatment allows further maturation of blood vessels while inducing adipogenesis in the model. In other published vascularized adipose tissue models, adipogenic cocktail treatments, e.g. insulin, IBMX, biotin, pantothenate, DEX and thiazolidinediones, have been proposed to have a negative effect on endothelial cells and delay the growth of HUVEC [18,29].

In this study, the co-cultures where angiogenesis structure was induced first (P2 and P6), tended to detach easier than the ones where adipogenesis was induced first (P1 and P5). This could problem could be addressed by coating the culture vessels. However, addition of external materials can cause unwanted and unknown interactions between the studied cells or chemicals assembly [23].

Effect of vasculature on adipocyte differentiation

Based on the commonly used adipogenesis markers *PPARγ, PPARγ2, leptin, adiponectin, Glut4* and *aP2* [27,30,31] adipogenic differentiation of hASC occurred in all protocols.

In addition, the gene expression results suggested that vasculature has a positive effect in adipocyte differentiation. There was a clear trend of higher expression of all the studied gene markers in the vascularized adipose model compared to the adipocyte control even though statistically significant difference was found only in adiponectin expression in protocol P1. The role of ECM produced by the hASC and the formed vascular structures in the culture is one important part of the model as it offers attachment places and support for differentiation of adipocytes [21]. The hASC and HUVEC vascular network has already been shown to produce ECM and Collagen IV containing basement membrane [26] and it and its role in adipogenesis should be studied further.

PPARγ expression is considered a general marker for ongoing adipogenesis and thus should be found in the adipocyte models [29,32]. *PPARγ2* is more adipocyte specific isoform of *PPARγ* [33,34] and it is transcriptionally regulated by nutrition [33,35]. *PPARγ2* has been found to be important for the storage of lipids in adipocytes in adipose tissue instead of other organs and hence its proper expression is highly important in obesity [36]. Our results support this and finding of Robciuc et al. [9] because the adipocytes in P6, which had extensive vasculature prior to adipogenesis induction, had strong expression of *PPARγ2* (Fig 4), and also the size of the lipid storage per cell was largest of the studied protocols (Fig 2). This is an interesting finding and should be studied further.

Leptin and adiponectin, the most abundant secretory products of adipose tissue [37], are typically investigated when studying the secretory properties of the formed adipose tissue [30]. In our models, the expression of *leptin* was elevated implying that functional adipose tissue was formed. P1 adipocytes, which showed strong lipid accumulation, were also secreting leptin, indicating the saturated state of the adipocytes.

aP2 (also known as fatty acid-binding protein 4) regulates the lipid trafficking and response in cells [38]. Along with *aP2,* the glucose transporter Glut4 has been connected to the terminal stage of differentiation in 3T3-L1 cells [32]. As angiogenesis medium includes insulin, which increases glucose influx through Glut4 and represses lipolysis in adipocytes [39,40], it is possible that the combination of ATE and angiogenesis media treatments enhances adipose tissue maturation more than just ATE treatment in adipocyte control. Activated endothelial cells in angiogenic vessels are known to produce various cytokines and growth factors that promote adipose tissue growth and expansion [41].

According to our findings, one week of adipogenesis induction was enough to produce mature adipocytes if there was a dense and mature blood vessel network present prior to induction of adipogenesis, i.e., vasculature was enabling a faster differentiation of adipocytes. This was seen from the gene expression results, which did not differ significantly regardless of whether the adipocytes had two weeks (P1 and P5) or one week (P2 and P6) to mature in the culture. The positive effect of vasculature on adipose tissue has also been shown in mouse models by others [9,10], and hence it should be studied further to reveal the underlying mechanisms of the interaction of vasculature and adipocytes. This model provides a useful tool for studying these mechanisms and the role of vasculature on the adipocyte differentiation.

Technical aspects in model development

When developing a multicellular tissue model with relatively thick structures, gaining adequate and reproducible cell adherence might be difficult. This essential feature largely defines the applicability and repeatability of the otherwise functional model. According to our results, plating density had the strongest impact on the adherence of the cell model.

Fetal calf serum is the standard component of the present test models although it might have unpredicted effects during the culture. In addition to the lot-to-lot variation, proteins in fetal serum may bind studied compounds and affect the results obtained [42]. Therefore, the ultimate goal is to use serum-free medium whenever possible. In our model, the defined serum-free medium is present for 7 days in the culture. This makes the model less vulnerable to batch variation and other unknown protein interactions.

Cells of human origin should be used when studying human effects especially when metabolism of test substances might play a role [43-45]. However, only a few human cell based adipose tissue models have been developed so far [46]. Primary human cells utilized in this model might contain lot-to-lot variation and thus cause difficulties in standardization. However, the variation can be minimized by preset quality control procedures which includes verification of sufficient expression of prominent markers for each cell type used, e.g. CD73, CD90 and CD105 for hASC [26] and morphological monitoring of the cells.

Conclusions

As obesity is a severe and growing global problem, there is an urgent need for well-characterized, functional and relevant human *in vitro* models, which could be used in safety testing of chemicals, in drug development as well as in biomedical research of healthy and disease modelling tissue. Also new legislations, such as REACH are increasing the demand of in vitro models. This study provides new information on combining two components; vasculature and adipocytes, in culture and led to development of novel *in vitro* model for adipose tissue studies. Both angiogenesis and adipogenesis were successfully induced in the co-culture with the protocols used in this

study. Presence of mature vasculature showed to be beneficial; it appears to lead to further maturation of preadipocytes and adipocytes. The underlying mechanisms of this interaction should be studied further as they might provide a target for therapeutic strategies.

The next step is to show with a set of reference chemicals the applicability of the model for chemical testing on adipogenesis but even now, the model is ready to be used for adipose tissue research when e.g. studying the effect of different cell types on adipose tissue function or for mechanistic studies.

Acknowledgements

We thank the treating staff at the Tampere University Hospital as well as the donors for the umbilical cords and adipose tissue samples. We thank Ms Sari Leinonen, Ms Paula Helpiölä, Ms Mirja Hyppönen for technical assistance. Funding for the project was kindly provided by the Diabetes Research Foundation, Paavo Nurmi foundation, Ministry of Education and Culture and Ministry of Agriculture and Forestry.

References

[1] Cavan D, da Rocha Fernandes J, Makaroff L, Ogurtsova K, Webber S editors. IDF Diabetes Atlas. 7th ed. Brussels, Belgium: International Diabetes Federation; 2015.

[2] Al-Awar A, Kupai K, Veszelka M, Szucs G, Attieh Z, Murlasits Z, et al. Experimental Diabetes Mellitus in Different Animal Models. J Diabetes Res 2016;2016:9051426.

[3] Heinonen T. Better science with human cell-based organ and tissue models. Altern Lab Anim 2015 Mar;43(1):29-38.

[4] Chandrasekera PC, Pippin JJ. Of rodents and men: species-specific glucose regulation and type 2 diabetes research. ALTEX 2014;31(2):157-176.

[5] European Union. Directive 2010/63/EU of the European Parliament and of the Council of 22 September 2010 on the protection of animals used for scientific purposes. Official Journal of the European Union 2010;L276:33-79.

[6] European Union. Regulation (EC) No 1223/2009 of the European Parliament and of the Council of 30 November 2009 on cosmetic products. Official Journal of the European Union 2009;L342:59-209.

[7] European Union. Commission Regulation (EC) No134/2009 of 16 February 2009 amending Regulation (EC) No 1907/2006 of the European Parliament and of the Council on the Registration, Evaluation, Authorisation and Restriction of Chemicals (REACH) as regards Annex XI. Official Journal of the European Union 2009;L46:3–5.

[8] Christiaens V, Lijnen HR. Angiogenesis and development of adipose tissue. Mol Cell Endocrinol 2010 Apr 29;318(1-2):2-9.

[9] Robciuc MR, Kivela R, Williams IM, de Boer JF, van Dijk TH, Elamaa H, et al. VEGFB/VEGFR1-Induced Expansion of Adipose Vasculature Counteracts Obesity and Related Metabolic Complications. Cell Metab 2016 Apr 12;23(4):712-724.

[10] Rupnick MA, Panigrahy D, Zhang CY, Dallabrida SM, Lowell BB, Langer R, et al. Adipose tissue mass can be regulated through the vasculature. Proc Natl Acad Sci U S A 2002 Aug 6;99(16):10730-10735.

[11] Corvera S, Gealekman O. Adipose tissue angiogenesis: impact on obesity and type-2 diabetes. Biochim Biophys Acta 2014 Mar;1842(3):463-472.

[12] Pasarica M, Sereda OR, Redman LM, Albarado DC, Hymel DT, Roan LE, et al. Reduced adipose tissue oxygenation in human obesity: evidence for rarefaction, macrophage chemotaxis, and inflammation without an angiogenic response. Diabetes 2009 Mar;58(3):718-725.

[13] Trayhurn P. Hypoxia and adipose tissue function and dysfunction in obesity. Physiol Rev 2013 Jan;93(1):1-21.

[14] Hausman GJ, Richardson RL. Adipose tissue angiogenesis. J Anim Sci 2004 Mar;82(3):925-934.

[15] Hoying JB, Utzinger U, Weiss JA. Formation of microvascular networks: role of stromal interactions directing angiogenic growth. Microcirculation 2014 May;21(4):278-289.

[16] Du P, Subbiah R, Park JH, Park K. Vascular morphogenesis of human umbilical vein endothelial cells on cell-derived macromolecular matrix microenvironment. Tissue Eng Part A 2014 Sep;20(17-18):2365-2377.

[17] Rhodes JM, Simons M. The extracellular matrix and blood vessel formation: not just a scaffold. J Cell Mol Med 2007 Mar-Apr;11(2):176-205.

[18] Kang JH, Gimble JM, Kaplan DL. In vitro 3D model for human vascularized adipose tissue. Tissue Eng Part A 2009 Aug;15(8):2227-2236.

[19] Borges J, Muller MC, Momeni A, Stark GB, Torio-Padron N. In vitro analysis of the interactions between preadipocytes and endothelial cells in a 3D fibrin matrix. Minim Invasive Ther Allied Technol 2007;16(3):141-148.

[20] Borges J, Mueller MC, Padron NT, Tegtmeier F, Lang EM, Stark GB. Engineered adipose tissue supplied by functional microvessels. Tissue Eng 2003 Dec;9(6):1263-1270.

[21] Sorrell JM, Baber MA, Traktuev DO, March KL, Caplan AI. The creation of an in vitro adipose tissue that contains a vascular-adipocyte complex. Biomaterials 2011 Dec;32(36):9667-9676.

[22] Norotte C, Marga FS, Niklason LE, Forgacs G. Scaffold-free vascular tissue engineering using bioprinting. Biomaterials 2009 Oct;30(30):5910-5917.

[23] Williams DF. On the mechanisms of biocompatibility. Biomaterials 2008 Jul;29(20):2941-2953.

[24] Higgins SP, Solan AK, Niklason LE. Effects of polyglycolic acid on porcine smooth muscle cell growth and differentiation. J Biomed Mater Res A 2003 Oct 1;67(1):295-302.

[25] Sarkanen JR, Kaila V, Mannerstrom B, Raty S, Kuokkanen H, Miettinen S, et al. Human adipose tissue extract induces angiogenesis and adipogenesis in vitro. Tissue Eng Part A 2012;18(1-2):17-25.

[26] Huttala O, Vuorenpaa H, Toimela T, Uotila J, Kuokkanen H, Ylikomi T, et al. Human vascular model with defined stimulation medium - a characterization study. ALTEX 2015;32(2):125-136.

[27] Huttala O, Mysore R, Sarkanen JR, Heinonen T, Olkkonen VM, Ylikomi T. Differentiation of human adipose stromal cells in vitro into insulin-sensitive adipocytes. Cell Tissue Res 2016;366(1):63-74.

[28] Sarkanen JR, Vuorenpaa H, Huttala O, Mannerstrom B, Kuokkanen H, Miettinen S, et al. Adipose stromal cell tubule network model provides a versatile tool for vascular research and tissue engineering. Cells Tissues Organs 2012;196(5):385-397.

[29] Foley B, Clewell R, Deisenroth C. Development of a human adipose-derived stem cell model for characterization of chemical modulation of adipogenesis. Applied In Vitro Toxicology 2015;1(1):66-78.

[30] Choi JH, Gimble JM, Lee K, Marra KG, Rubin JP, Yoo JJ, et al. Adipose tissue engineering for soft tissue regeneration. Tissue Eng Part B Rev 2010;16(4):413-426.

[31] Zhou Y, Robciuc MR, Wabitsch M, Juuti A, Leivonen M, Ehnholm C, et al. OSBP-related proteins (ORPs) in human adipose depots and cultured adipocytes: evidence for impacts on the adipocyte phenotype. PLoS One 2012;7(9):e45352.

[32] Gregoire FM, Smas CM, Sul HS. Understanding adipocyte differentiation. Physiol Rev 1998;78(3):783-809.

[33] Ren D, Collingwood TN, Rebar EJ, Wolffe AP, Camp HS. PPARgamma knockdown by engineered transcription factors: exogenous PPARgamma2 but not PPARgamma1 reactivates adipogenesis. Genes Dev 2002;16(1):27-32.

[34] Escher P, Braissant O, Basu-Modak S, Michalik L, Wahli W, Desvergne B. Rat PPARs: quantitative analysis in adult rat tissues and regulation in fasting and refeeding. Endocrinology 2001;142(10):4195-4202.

[35] Werman A, Hollenberg A, Solanes G, Bjorbaek C, Vidal-Puig AJ, Flier JS. Ligand-independent activation domain in the N terminus of peroxisome proliferator-activated receptor gamma (PPARgamma). Differential activity of PPARgamma1 and -2 isoforms and influence of insulin. J Biol Chem 1997;272(32):20230-20235.

[36] Medina-Gomez G, Gray SL, Yetukuri L, Shimomura K, Virtue S, Campbell M, et al. PPAR gamma 2 prevents lipotoxicity by controlling adipose tissue expandability and peripheral lipid metabolism. PLoS Genet 2007;3(4):e64.

[37] Coelho M, Oliveira T, Fernandes R. Biochemistry of adipose tissue: an endocrine organ. Arch Med Sci 2013;9(2):191-200.

[38] Furuhashi M, Saitoh S, Shimamoto K, Miura T. Fatty acid-binding protein 4 (fabp4): pathophysiological insights and potent clinical biomarker of metabolic and cardiovascular diseases. Clin Med Insights Cardiol 2015;8(Suppl 3):23-33.

[39] Watson RT, Pessin JE. GLUT4 translocation: the last 200 nanometers. Cell Signal 2007;19(11):2209-2217.

[40] Choi SM, Tucker DF, Gross DN, Easton RM, DiPilato LM, Dean AS, et al. Insulin regulates adipocyte lipolysis via an Akt-independent signaling pathway. Mol Cell Biol 2010;30(21):5009-5020.

[41] Cao H. Adipocytokines in obesity and metabolic disease. J Endocrinol 2014;220(2):T47-59.

[42] Shen Q, Wang L, Zhou H, Jiang HD, Yu LS, Zeng S. Stereoselective binding of chiral drugs to plasma proteins. Acta Pharmacol Sin 2013;34(8):998-1006.

[43] Ginis I, Luo Y, Miura T, Thies S, Brandenberger R, Gerecht-Nir S, et al. Differences between human and mouse embryonic stem cells. Dev Biol 2004;269(2):360-380.

[44] Mestas J, Hughes CC. Of mice and not men: differences between mouse and human immunology. J Immunol 2004;172(5):2731-2738.

[45] Rangarajan A, Weinberg RA. Opinion: Comparative biology of mouse versus human cells: modelling human cancer in mice. Nat Rev Cancer 2003;3(12):952-959.

[46] Ruiz-Ojeda FJ, Ruperez AI, Gomez-Llorente C, Gil A, Aguilera CM. Cell models and their application for studying adipogenic differentiation in relation to obesity: a review. Int J Mol Sci 2016;17(7):1040.

[47] Shepherd PR, Kahn BB. Glucose transporters and insulin action--implications for insulin resistance and diabetes mellitus. N Engl J Med 1999;341(4):248-257.

[48] Rosen ED, Sarraf P, Troy AE, Bradwin G, Moore K, Milstone DS, et al. PPAR gamma is required for the differentiation of adipose tissue in vivo and in vitro. Mol Cell 1999;4(4):611-617.

[49] Tontonoz P, Hu E, Graves RA, Budavari AI, Spiegelman BM. mPPAR gamma 2: tissue-specific regulator of an adipocyte enhancer. Genes Dev 1994;8(10):1224-1234.

TABLES and FIGURES

Table 1. Plating and differentiation details of different protocols tested on hASC-HUVEC co-cultures.

Protocol name	hASC plating day(s)	Number of hASC/well	HUVEC plating day	Number of HUVEC /well	Medium on days 1-7	Medium on days 8-14
P1	Day 0 Day 7	22 000 cells 22 000 cells	Day 7	4400 cells	ATE medium	Angiogenesis medium
P2	Day 0 Day 7	22 000 cells 22 000 cells	Day 0	4400 cells	Angiogenesis medium	ATE medium
P3	Day 0	44 000 cells	Day 0	4400 cells	ATE medium	Angiogenesis medium
P4	Day 0	44 000 cells	Day 0	4400 cells	Angiogenesis medium	ATE medium
P5	Day 0	22 000 cells	Day 0	4400 cells	ATE medium	Angiogenesis medium
P6	Day 0	22 000 cells	Day 0	4400 cells	Angiogenesis medium	ATE medium
Negative control	Day 0	44 000 cells	Day 0	4400 cells	Serum-free Basic medium	Serum-free Basic medium
Vasculature control	Day 0	22 000 cells	Day 0	4400 cells	Angiogenesis medium	Angiogenesis medium
Adipocyte control	Day 0	22 000 cells	-	-	ATE medium	ATE medium

Table 2. Composition of differentiation media used in the study.

Medium	Components	Manufacturer
ATE medium	DMEM/F-12 1800µg/ml ATE 10 % Human Serum 2 mM L-Glutamine 50 units/µl Penicillin-50 µg/µl Streptomycin	Gibco PAA Laboratories Gibco Gibco
Serum-free Basic medium	DMEM/F-12 1 % Bovine Serum Albumin (BSA) 2.8 mM Sodium Puryvate 2.56 mM L-Glutamine ITS-supplement: 6.65 µg/ml Insulin 6.65 µg/ml Transferrin 6.65 ng/ml Selenious	Gibco Biosera (Boussens, France) Gibco Gibco BD Biosciences (NJ, USA)

	0.1 nM 3,3,5-Triiodo-L-thyronine sodium salt	Sigma Aldrich (MO, USA)
Angiogenesis medium	Serum-free medium 200 µg/ml Ascorbic Acid 2 µg/ml Hydrocortisone: 1 ng/ml FGF-β 10 ng/ml VEGF 0.5 µg/ml Heparin	 Sigma Aldrich Sigma Aldrich R&D Systems (Abingdon, UK) R&D Systems Sigma-Aldrich

Table 3 Studied genes and the primer sequences used.

Gene name	Abbreviation	Primer sequence (5'→ 3')	Function
Succinate dehydrogenase complex, subunit A	SDHA	F: CATGCTGCCGTGTTCCGTGTGGG R: GGACAGGGTGTGCTTCCTCCAGTGCTCC	Used as a housekeeping gene in this study
Acidic ribosomal phosphoprotein P0	36B4	F: ATGCTCAACATCTCCCCCTTCTCC R: GGGAAGGTGTAATCCGTCTCCACAG	Used as a housekeeping gene in this study
Leptin	-	F: GCCCTATCTTTTCTATGTCC R: TCTGTGGAGTAGCCTGAAG	Adipose tissue secretory product [37]
Adiponectin	-	F: GGCCGTGATGGCAGAGAT R: CCTTCAGCCCGGGTACT	Adipose tissue secretory product [37]
Adipocyte protein 2 (fatty acid-binding protein 4)	AP2	F: GCTTTTGTAGGTACCTGGAAACTT R: ACACTGATGATCATGTTAGGTTTGG	Carrier protein for fatty acids [38]
Glucose transporter type 4	Glut4	F: TGGGCGGCATGATTTCCTC R: GCCAGGACATTGTTGACCAC	Insulin responsive glucose transporter [47]
Peroxisome proliferator-activated receptor γ	PPARγ	F: GATCCAGTGGTTGCAGATTACAA R: GAGGGAGTTGGAAGGCTCTTC	Transcription factor in adipogenesis [48]
Peroxisome proliferator-activated receptor γ variant 2	PPARγ2	F: CAGTGTGAATTACAGCAAACC R: ACAGTGTATCAGTGAAGGAAT	Transcription factor in adipogenesis, adipocyte-specific variant [49]

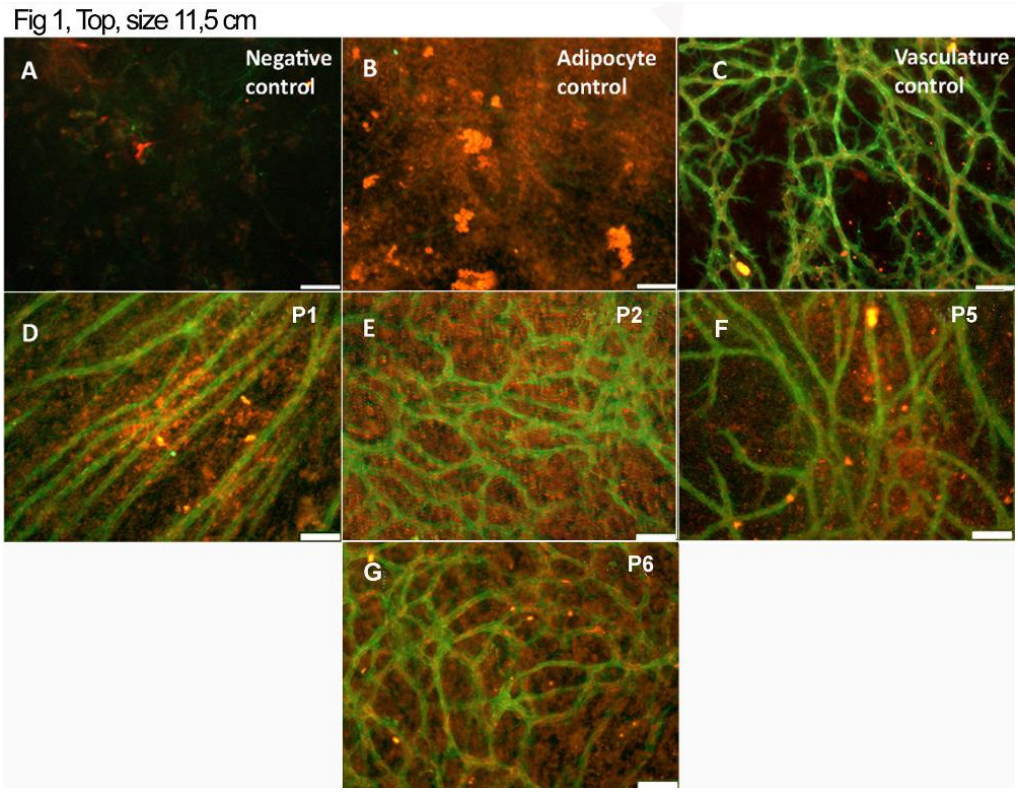

Fig 1. Morphology of the vascularized adipose tissue models on day 14. Lipids are seen in orange/red, tubules are stained with anti-vWF-TRITC (red) and anti-ColIV- FITC (green). (**A)** Negative control (**B)** Adipocyte control with strong adipored staining (**C)** Vasculature control with strong tubule network (**D)** P1 produced tubules but only few branches. Adipored staining showed strong lipid staining within the cells. (**E)** P2 produced well branched tubule network and evenly spread adipored staining. (**F)** P5 produced dense tubule network but it was less dense than with (**G)** the protocol 6. Both P5 and P6 show good adipored staining. Images are obtained with Nikon Eclipse Ti-S inverted fluorescence microscope and with 10x objective, scale bar is 100 µm.

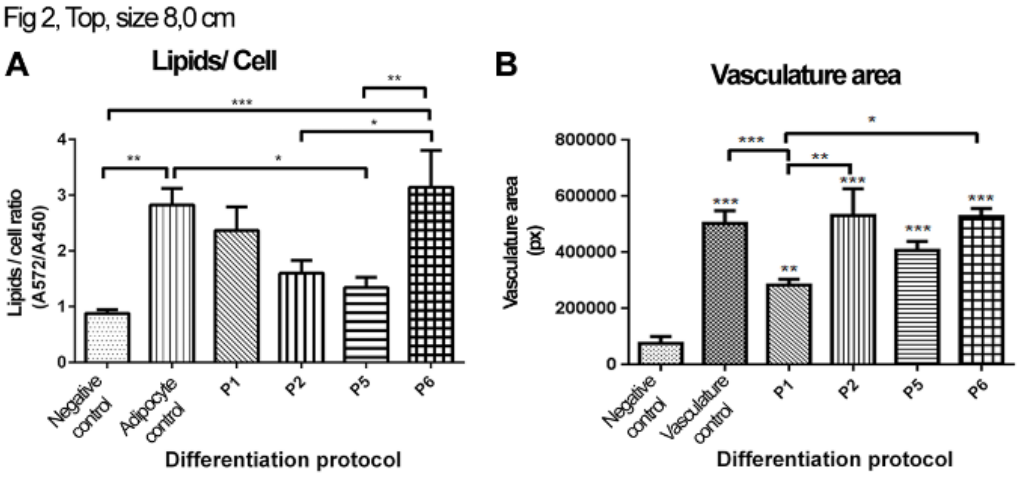

Fig 2. Lipid accumulation and area of vasculature in the vascularized adipose tissue models on day 14. (**A)** Adipocyte control and all protocols show lipid accumulation, P5 was the only one, which accumulated significantly less lipids than the adipocyte control. (**B)** All protocols produced dense tubular network except P1, which formed significantly less tubules compared to the vasculature control, P2 and P6. The bars represent mean±SD. *n* was 12 except for P5 and P6 for which the *n* was 5 due to detachment. *p<0.05, **p<0.01and ***p<0.001.

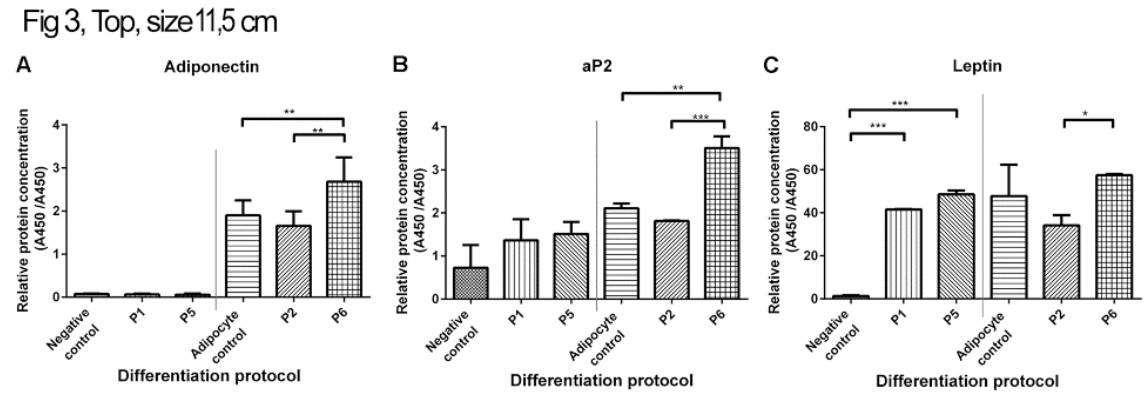

Fig 3. Protein secretion of adipocytes in the studied protocols. Adipocyte control and P2 and P6 contain cytokine rich ATE and hence their results were compared to each another whereas negative control, P1 and P5 were compared to each other. (**A)** Secretion of adiponectin was significantly increased in P6 compared to adipocyte control and P2. (**B)** aP2 was secreted significantly more in P6 than in the adipocyte control and P2. (**C)** Secretion of leptin was

significantly higher in P1 and P5 than in the negative control, and also higher in P6 than P2. The bars represent mean±SD. For lipid accumulation *n* was 15 and for ELISA *n* was 3. *p<0.05, **p<0.01and ***p<0.001.

Fig4, Top, size 8,0 cm

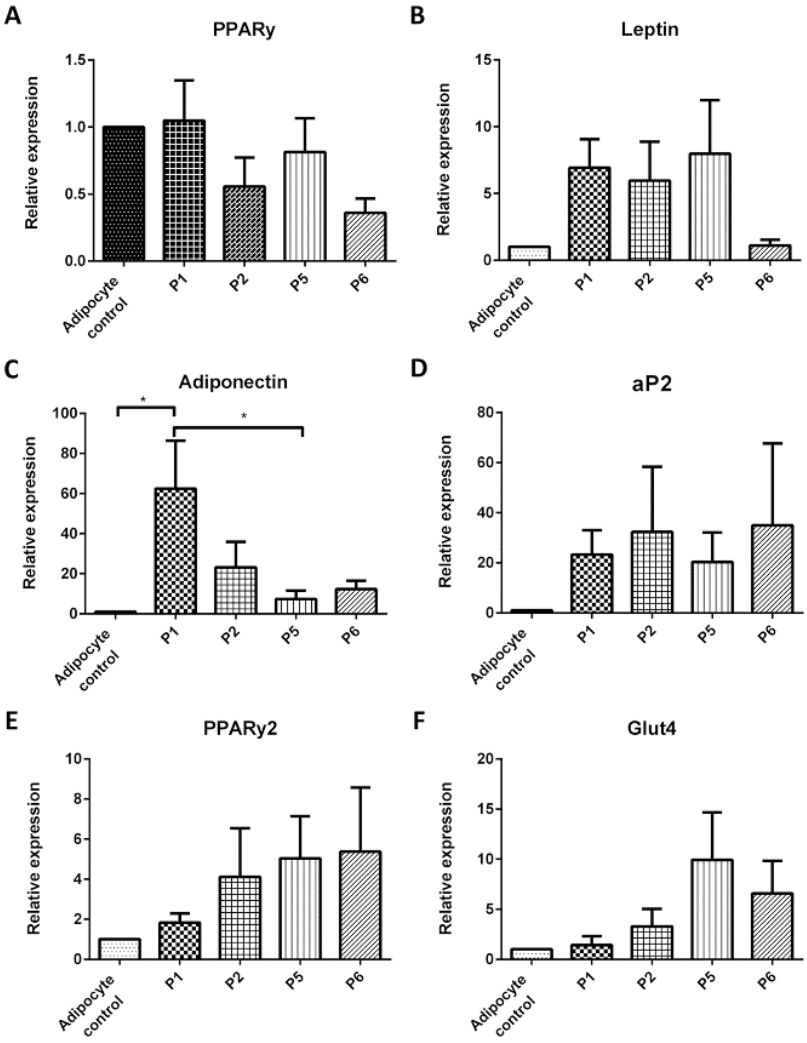

Fig 4. The expression of adipose tissue specific gene markers in the studied protocols. (A) *PPARγ* **(B)** *Leptin* (**C)** *Adiponectin* (**D)** *aP2* (**E)** *PPARγ2* (**F)** *Glut4*. P1 showed significantly increased expression of *adiponectin* compared to adipocyte control and P5. The bars represent mean with SD. *n* was 4, *p<0.05.